Geologica Acta, Vol.13, Nº 2, June 2015, 85-96
DOI: 10.1344/GeologicaActa2015.13.2.1

geologicaacta

Long term recovery rates obtained using RFID technology at a mixed beach

M. CASAMAYOR[1*] I. ALONSO[1] J. CABRERA[2] S. RODRÍGUEZ[1] M.J. SÁNCHEZ-GARCÍA[1]

[1]Instituto de Oceanografía y Cambio Global. Universidad de Las Palmas de Gran Canaria.
Campus Universitario Tafira, 35017 Las Palmas de Gran Canaria.
Casamayor E-mail: marionacasamayor@gmail.com

[2]Instituto Universitario de Sistemas Inteligentes y Aplicaciones Numéricas en Ingeniería. Universidad de Las Palmas de Gran Canaria.
Campus Universitario de Tafira, 35017 Las Palmas de Gran Canaria.

ABSTRACT

Recovery rates were obtained by radio frequency identification (RFID) technology in pebbles and cobbles at San Felipe beach, Gran Canaria. The aim of this work was to define which factors affected the recovery of tagged gravels. Several tests were performed to determine the detection depth threshold, and 16 field experiments were carried out over seventeen months after tracer deployment on the beach. Recovery rates are highly variable with time, ranging from 72.2% in the first recovery session to 25.8% in the last one. Nevertheless, a nearly stable situation was found for the final eight months. Apart from the effect of time, there were several factors that affected the recovery rate. Some of these were related to the particle, such as the position of the tag within the particle, as well as its weight, size and shape. Two environmental factors were considered. First, the elevation of the tracer on the beach showed that the recovery rate was higher with particles located above the storm berm. Second, wave height, which showed no relation with recovery rates even though during the experiment significant storms and periods of calm took place.

KEYWORDS **Tracer recovery. Pebbles. Detection. Sediment transport. Gran Canaria.**

INTRODUCTION

Sediment transport is one of the fundamental aspects that must be addressed in order to understand the processes that take place on beaches, and it is therefore indispensable to properly manage these coastal areas. Sandy beaches have been studied for many years and there is much available information on the mechanisms of sediment transport. However, there are few studies on coarse-grained beaches due to the logistical difficulties involved, such as the rough dynamic conditions and the fragility of the instrumentation. One of the most important characteristics of coarse-grained beaches are their high efficiency at protecting shore from extreme wave conditions, due to their high degree of stability (Carter and Orford, 1984), so that in many places these beaches are considered as a management tool against coastal erosion (Allan and Komar, 2004; Dickson *et al.*, 2011). Interest in these kinds of beaches has increased thanks to technological advances that allow for the study of transport of individual particles over long periods of time (Allan *et al.*, 2006; Curtiss *et al.*, 2009; Bertoni *et al.*, 2010, 2012; Dickson *et al.*, 2011).

There are three predominant types of tracers (Allan *et al.*, 2006). The first group are visual tracers that consist of painted coarse-grained particles or exotic lithologies for the quick identification of the particles. Such tracers have different problems, such as those derived from their burial and the loss of paint with the pass of time. These problems lead to low recovery rates (between 5 and 50%)

(Joliffe, 1964; Dornbusch *et al.*, 2002; Sear *et al.*, 2002; Allan *et al.*, 2006; Ciavola and Castiglione, 2009). The second group are called passive tracers, and may include different techniques such as radioactive, aluminium, magnetic or electronic tracking technologies. These techniques are a significant improvement in tracking because they allow the user to locate particles even when they are buried. In this case, recovery rates show great variability, ranging from 40 to 85%, depending on the hydrodynamic conditions at the study area (Voulgaris *et al.*, 1999; Sear *et al.*, 2002; Osborne, 2005). Finally, the third group are active tracers which are composed of an electronic tracking system powered by a battery that is encapsulated within a resin to produce a tracer with the size and shape characteristic of beach particles (Bray *et al.*, 1996; Voulgaris *et al.*, 1999). The great advantage of these tracers is that they can be detected up to a depth of 1m, rising recovery rates to values greater than 70%. However, their drawbacks are their costs and artificial nature, which can influence the tracer response to local hydrodynamic conditions (Allan *et al.*, 2006).

The tracers used in this study are passive tracers, the radio frequency identification (RFID) tracers. This technique presents a high ratio of efficiency to cost, since it is possible to obtain high recovery rates with low operating costs (Allan *et al.*, 2006; Bertoni *et al.*, 2010).

This paper presents the results of applying RFID technology to the mixed beach of San Felipe, Gran Canaria, to study the recovery rates of pebbles and cobbles over one and a half year. The different factors that can affect the recovery rate are considered. Factors related to the tracer are weight, size, shape and the axis through which the tag is inserted; and those related to the environment are wave conditions and elevation of the tracer on the beach profile.

REGIONAL SETTING

The study area, San Felipe beach, is located on the north coast of the island of Gran Canaria (Spain), at the western limit of San Felipe village (Fig. 1). It is approximately 200m long and has variable width depending on the season, ranging from 20m wide in winter to 40m in summer, measured from the upper part of the beach profile to 0m orthometric height.

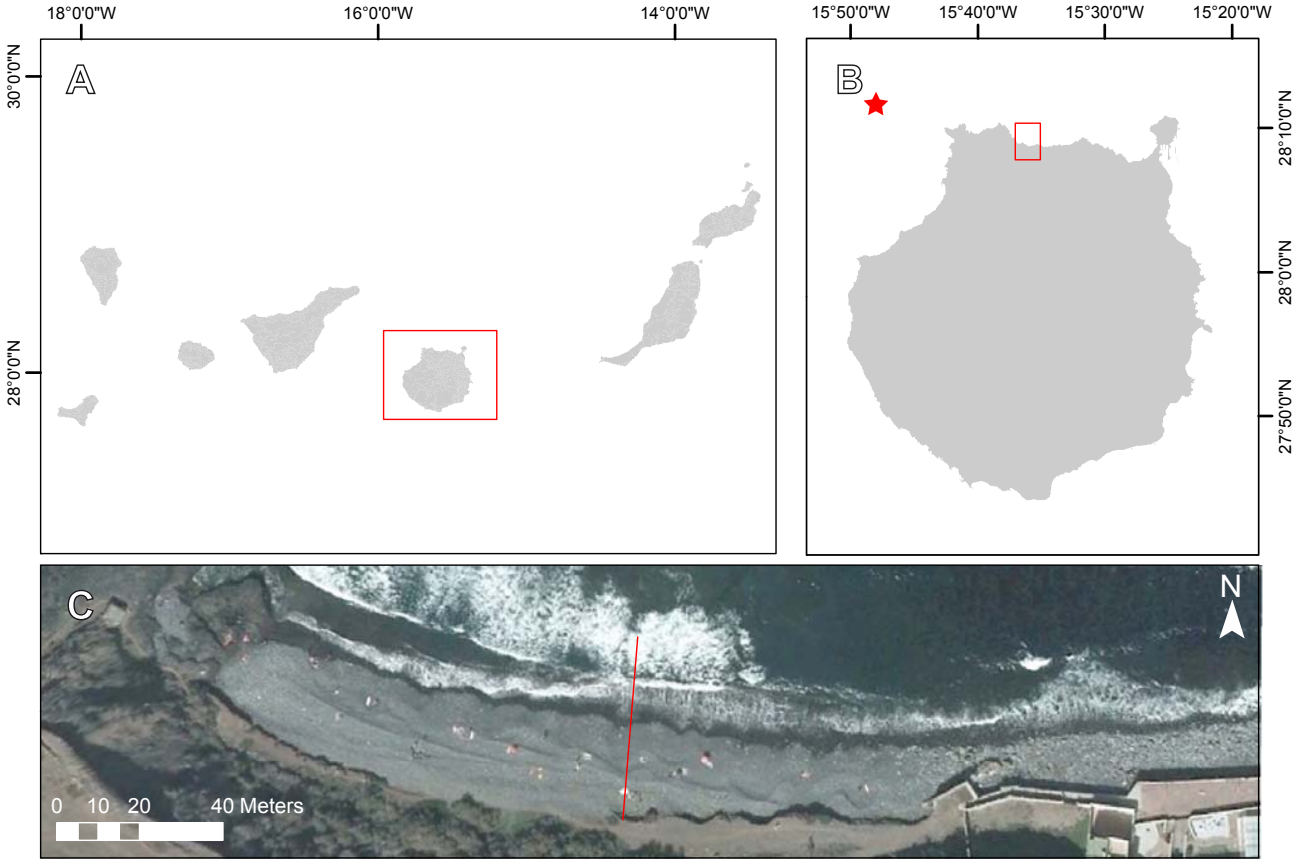

FIGURE 1. A) Map of Canary Islands. B) The star close to the island of Gran Canaria indicates the wave buoy location used in this work, and the square shows the location of the study area. C) Aerial photograph of San Felipe beach. The line is the beach profile shown in Figure 3.

San Felipe is a mixed beach consisting of fine black sand formed by basalt erosion (Balcells and Barrera, 1990), and coarse-grained particles that are mainly phonolitic and basaltic pebbles and cobbles. Coarse-grained materials are distributed over the backshore and upper foreshore, while sand is found on the lower foreshore and nearshore (Fig. 2). San Felipe beach is subjected to large morphological changes, which are mostly related to wave climate variations. In winter time, storm berm is formed, which increases the foreshore slope. During this season only cobbles and pebbles are visible along the beach, even at low tide. Around May, with the beginning of the trade winds, the submerged sand bar moves onshore, and by the end of the summer the cobbles and pebbles located on the foreshore become completely covered by sand, with a clear reduction in beach slope (Fig. 3).

In a general geological context, the northern coast of Gran Canaria is characterized by phonolitic Miocene lava flows that have been eroded by the sea, and constitute a coastal platform raised 6–15m above mean local sea level (Balcells and Barrera, 1990). Most of this coastal platform is covered by crops and villages. The beach is backed by colluvial deposits and debris. The western edge is bounded by a basaltic lava flow, which enters into the sea, while the eastern sector of the beach leads to the ravine of San Felipe, 8,600m in length and maximum 817m in height (Menéndez *et al*., 2008).

Gran Canaria has a semidiurnal tidal regime with 2.8m tidal range at spring tides and 0.8m at neap tides. These are all astronomic tidal values obtained from the WXTide32 program. Data from wave recorder buoy number 2442 from Puertos del Estado have been used to characterize the wave climate. This buoy is located northwest of Gran Canaria, several km offshore and at 780m water depth (see location in Fig. 1).

FIGURE 2. Photograph of San Felipe beach at low tide during summer conditions. Note i) that pebbles and cobbles are very well rounded and quite well sorted, and ii) the sand over the lower foreshore.

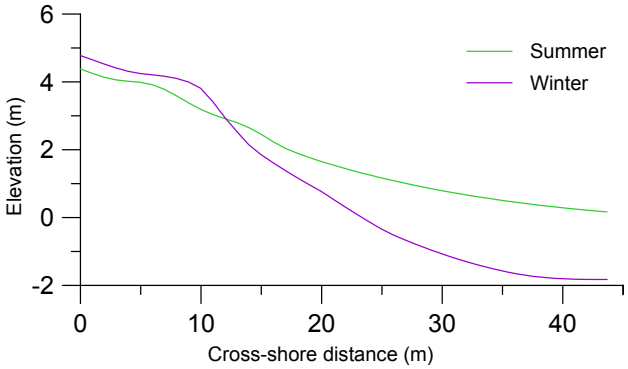

FIGURE 3. Beach profile at the central section of San Felipe beach. Profile location is shown in Figure 1C. Elevation corresponds to orthometric heights. Note the net accumulation of sediments in the summer profile, which is mostly related to the onshore migration of the sand bar.

Wave data covering the study period (from March 2013 to July 2014) are shown in Figure 4. Significant wave height (Hs), peak period (Tp) and wave direction show a clear seasonal pattern, with calm conditions from April to October and storm conditions from November to March. The first period is under the influence of the trade winds. Dominant waves come from the N–NNE, average Hs=1.52m and average Tp=9.43s. Regarding the winter season, dominant waves come from N, Hs=1.97m and Tp=12.08s. There are frequent storms that generate waves with Hs>4m. During the study period, 13 stormy events took place, all of them with Hs higher than 3.0m on average. The duration of these storms was highly variable, ranging from 7 to 71h.

METHODS

Particle sampling and preparation

To carry out the experiment 198 particles were collected over homogeneously distributed region along and across the beach. Sampling of pebbles and cobbles took place on November 1, 2012, at low spring tide conditions. Although sample selection was random, the particles had to meet certain requirements due to the limitations of the experiment: the major axis of the particle had to be larger than 42mm, and cobbles weighing more than 3kg were discarded. Considering these experimental limitations, axial lengths of 802 additional particles were measured in the beach to check if tracer dimensions were representative of beach particles. These 802 additional particles were randomly selected along and across the beach.

The three axes (long, intermediate and short) of each individual particle were measured by means of a vernier calliper with 0.1mm precision and weighed on a scale with precision of 0.01g.

Preparation of tracer particles was undertaken in three phases: drilling, tag introduction and sealing. The first phase consisted of drilling a hole of 6mm diameter and 40mm in length in each particle. Following Allan *et al.* (2006), Dickson *et al.* (2011) and Miller and Warrick (2012), the holes were drilled through the short-axis of the particle, but when it was smaller than 42mm, it was necessary to drill the hole through the intermediate-axis, or even through the major axis when the intermediate one did not reach the required length.

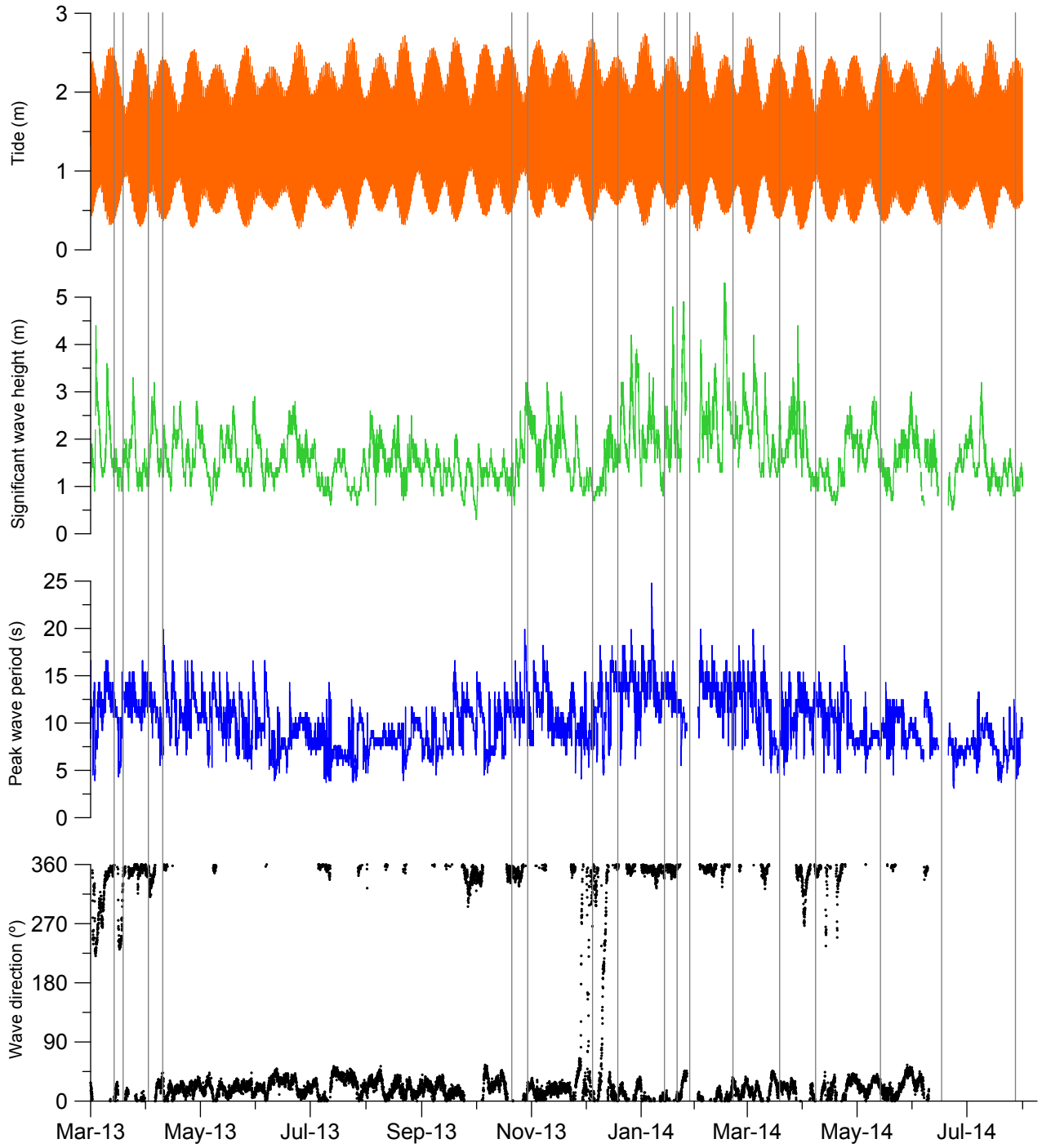

FIGURE 4. Hourly data recorded at the Gran Canaria buoy from March 2013 to August 2014. Tidal values were calculated with the WXTide32 program. Vertical lines show the date of the different field experiments.

The tag dimensions were 30.2±0.6mm long and 3.8±0.05mm in diameter and were protected by a glass capsule. To avoid breakage through impact with other coarse grains, tags were introduced into a plastic hose with a section of 4x6mm. Once this process was finished, both ends of the hose were sealed with universal acid silicone and the tag, properly protected, introduced into the cobble. Finally, the particles were sealed with epoxy resin of two components. This product was used because of its high resistance to impacts and temperature changes.

Tracers were regularly deployed on the beach on March 14, 2013 at low spring tide. The entire beach was surveyed sixteen times from March 19, 2013 to July 28, 2014 with a detection system to locate the tagged particles.

Detection system

This study uses RFID technology following Allan *et al.* (2006), who investigated a mixed sand and gravel beach with this method. The detection system is composed of a base station and one mobile detection device. The different elements of this system are listed on Table 1. Once a certain tag is detected, its identification number is stored in a micro SD card by the mobile device and transmitted to the base station in real time using a XBee radio module operating in the 869MHz ISM (Industrial. Scientific and Medical) radio band. Tracer positioning was carried out by means of an electronic total station.

The detection range of the RFID reader increases with supplied voltage. However, a high voltage generates heat that must be removed from the box that contains the electronic components. After experimenting with various voltages, it was found that 18V gave the best result, so that the detector temperature was kept within reasonable limits and the detection distance was close to the maximum.

The antenna is a circular structure of PVC tube 80cm in diameter containing a 1.88mm copper wire looped around three times. A synchronization module was used to adjust the radio frequency circuit to the resonant frequency of the antenna. When it detects a tag, the mobile detection device emits an acoustic signal and then its position is recorded by the total station.

TABLE 1. Summary of the different components that form the detection system.

SYSTEM	SUB-SYSTEM	COMPONENTS
Base station	Waspmote	12 channels SirFIII GPS receiver and radio modem XBee 868 Pro
	Laptop	With direct USB connections to waspmote
	Total station	
Mobile device	Battery 24V	12V/7Ah lead-gel batteries
	RFID reader	RI-CTL-MB2B from Texas Instruments
	RFM module	RI-RFM-008B from Texas Instruments
	Synchronization module	RI-ACC-008B from Texas Instruments
	Antenna	In-house design
	Waspmote	12 channels SirFIII GPS receiver and radio modem XBee 868 Pro
	RS232-3V3 adapter	

Detection range

Several tests were carried out in order to determine the maximum detection depth of our antenna. Considering that the beach under study contains different types of sediment, such as sand at the lower foreshore and cobbles and pebbles at the backshore, as well as water if the beach becomes submerged, some experiments were designed to assess the detection capability of the antenna in these three different media. In each medium, a tracer was buried at different depths, being the maximum detection depth considered the detection threshold. The relative position of the tag was considered: the tag could be perpendicular to the beach surface (which means that it was parallel to the short-axis of the pebble) or parallel to the surface (which may happen when the tag is either in the intermediate or in the long-axis).

TRACER CHARACTERISTICS

Since this work mostly deals with recovery rates of tracers, it is necessary to know the properties of these particles.

Weight

Tracer weight ranges between 82 and 2,837g with an average of 450.58g. These values were obtained once the particles had been drilled, the tag inserted and the hole sealed. Due to the large range of weights, it was necessary to make a transformation of the data. We chose the same transformation used by Krumbein (1936), who established the phi (Ø) scale for grain size. The proposed scale for particle weight is named phi-weight (Øw), and is defined as

$$Øw = log_2(W) \quad \text{W the particle weight in grams} \qquad (1)$$

After applying the above transformation and considering that the different categories derived from the Øw scale are delimited by integer units, all our tracers lay in the small range between 6 and 12Øw. There are two main categories (7–8 and 8–9Øw) of very similar abundances, with the average value corresponding to 8.82Øw, equivalent to 450.58g (Fig. 5A).

The weight loss during preparation of the tracer was calculated measuring the initial and final weight of three particles. The final weight takes into account the drilling, the introduction of the tag and sealing of the hole. Table 2 shows that the preparation process represents an average

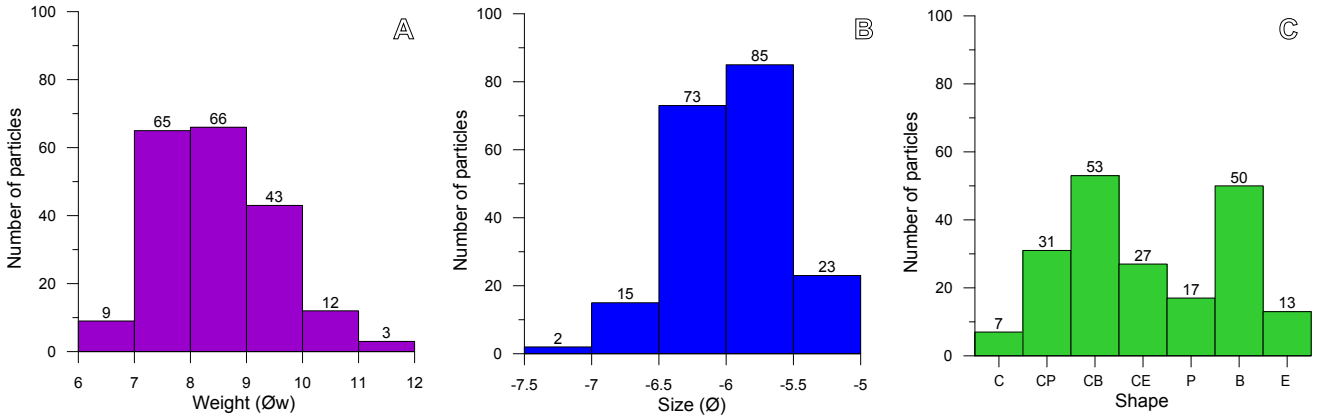

FIGURE 5. A) Distribution of tracer weights using the Øw scale. B) Distribution of tracer sizes, in Ø. C) Distribution of tracer shapes according to the Sneed and Folk (1958) classification (C: compact, P:platy, B:bladed, E:elongate).

mass loss of 0.58% of the initial weight for these three particles. Considering that these particles are lighter than the average, and that the weight loss is similar in each particle and does not depend on its size, the estimate average loss of weight of the whole of the particles is only 0.42%.

Size

Tracer particle size is in the range of cobbles and pebbles. The major axis ranges between 49.2 to 160.0mm, with an average length of 85.73mm, the intermediate axis is in the range 42.5–135.0mm, with an average length of 65.28mm, and the minor axis measures between 26.0 and 90.0mm (average length of 44.70mm).

Figure 6 shows the three axis length distribution for two types of particles: those used as tracers (198 particles) and 802 additional particles whose axes were measured. It is shown that both populations follow a normal distribution with regard to any of the three axes. Note that the distribution of the three axes in the tracer population is very similar to that in the population of 802 particles, and therefore it is very reasonable to assume that the selected pebbles and cobbles used as tracers are representative of the particles on the beach.

TABLE 2. Morphometric properties and weight of selected particles used to determine weight loss resulting from the preparation of the tracers.

PARTICLE ID	AXIS			WEIGHT		
	SHORT (mm)	INTERMEDIATE (mm)	LONG (mm)	INITIAL (g)	FINAL (g)	LOSS (%)
175	48	64.0	78.5	308.06	306.25	0.59
176	42	65.5	83.5	345.11	343.06	0.59
177	44	65.1	80.6	336.94	335.09	0.55
Average 3 particles	44.67	64.87	80.87	330.04	328.13	0.58
Average 198 particles	44.71	65.28	85.73	452.48	450.58	0.42

In fact, the average grain size is -5.95Ø and -5.78Ø for the tracer population and for the additional 802 beach particles respectively. Considering the intermediate axis as the average particle size, the dominant size of tracers corresponds to very coarse pebbles (between -5.5 to -6.0Ø), based on the Blair and McPherson (1999) classification (Fig. 5B).

Shape

The shape of the particles was analysed using the approach of Sneed and Folk (1958) based on the ratio between their three axes. Figure 7 shows the predominant shapes of 1000 particles plotted on the diagram proposed by Sneed and Folk (1958). There are slight differences between additional beach particles and tracers. In most parts of the beach particles are bladed, and tracers are either bladed or compact-bladed (Fig. 5C). Moreover, tracers are not very-platy, very-bladed or very-elongate since these categories are not suitable for particle preparation.

RESULTS

Detection threshold

Several tests were performed on the beach to determine the detection threshold of the system. Table 3 shows that the greatest detection depth occurs when the tag is buried in gravel decreases in the case of sand, and has the lowest values when it is immersed in water. These results confirm that the propagation of electromagnetic waves in water is worse than in solid media. On the other hand, the detection range is greater when the tags are in the short-axis of the pebbles, which is the direction normal to the electromagnetic field generated by the antenna, while the lowest range occurs when the tags are in the long-axis.

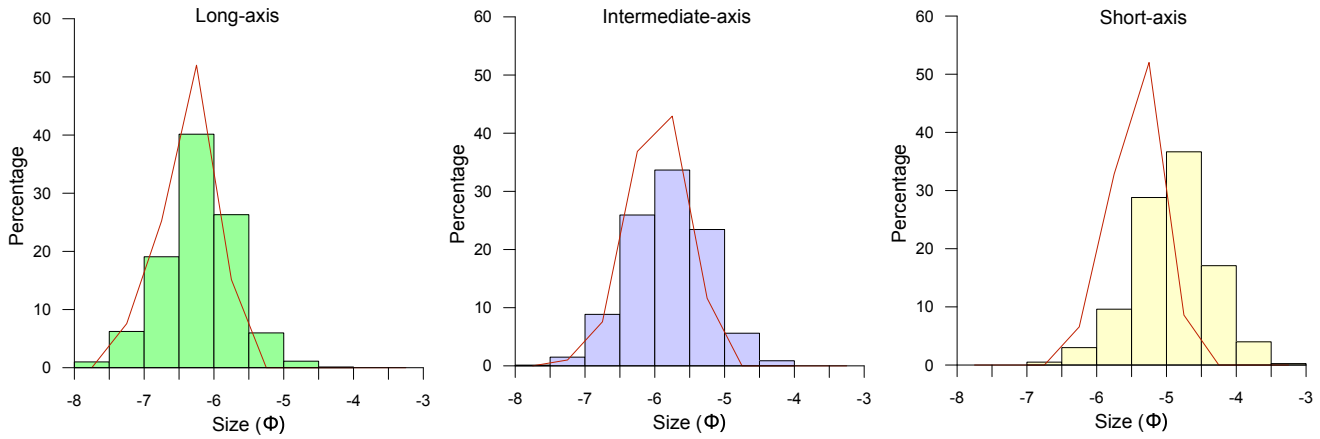

FIGURE 6. Axis length distributions for both populations: 198 particles used as tracers (lines) and 802 particles whose axes were measured (histograms).

Tracer recovery

Sixteen field experiments covering the period between March 2013 and July 2014 were carried out to determine the movement of the tracers on the beach. The number of tracers recovered (detected by RFID system) shows a clear decrease with time, so that the longer the elapsed time between the deployment and recovery, the lower the amount of tagged particles recovered (Fig. 8). In fact, during the first field session carried out five days after deployment (March 19th), only 143 tracers from 198 were found, and three weeks later the number had decreased to 114. From these numbers it could be guessed that in three months all tracers should have been removed, but what we really found was that nearly 18 months later there were still 51 tracers left on the beach. In fact, the cloud of dots (Fig. 8) may be fitted by a linear trend, which indicates that the total disappearance of tracers would happen by March 2015 (two years after deployment), or by an exponential fit in which case two and a half years after deployment we still should have 10% of the initial number of tracers.

Factors related to the tracer

The tag may be inserted into the particle through the long, intermediate or the short axis. The influence of this factor on the recovery rate is shown in Figure 9, from which it is clear that the number of recovered particles decreases with time for the three axes. Nevertheless, the linear fits (Fig. 9) clearly indicate that the particles in which the tag was inserted through the short-axis lasted longer compared to those particles with the tag in the intermediate or long axis. It should be noted that the initial number of tracers is not the same for each category. Tags in the long axis occur in only 27 particles, while there are 97 with the tag in the intermediate axis and 74 in the short axis. Relative to these numbers, the percentage of recovered particles with the tag in the short-axis is 37.8%, 36.7% in the intermediate-axis and 35% in the long-axis. These values confirm that the best position in terms of recovery is when the tag is inserted through the short-axis.

Regarding the weight of the particles, recovery rates of all categories of Øw (light, medium and heavy clasts) decrease with time. Nevertheless, particles with Øw between 7 and 8 (128–256g) have a higher negative slope, which indicates that this category will disappear sooner than the others (Fig. 10).

Recovery rates versus time and size of the pebbles and cobbles show similar patterns to those described for weight. The dominant categories of the initial 198 particles

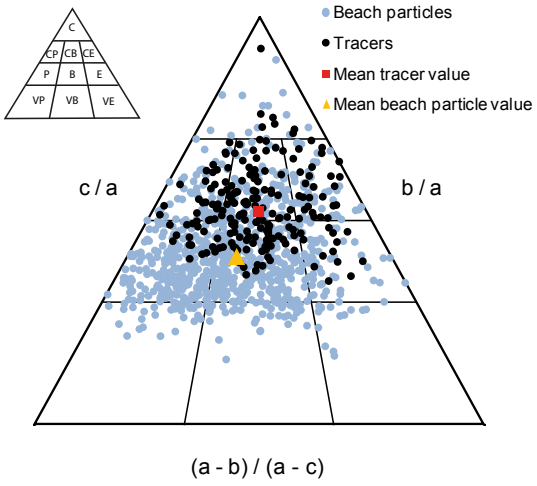

FIGURE 7. Tri-plot diagram based on Sneed and Folk (1958), which represents particle shapes according to their orthogonal axes: 198 tracers, and 802 additional beach particles. a: long-axis, b: intermediate-axis, c: short-axis. C: compact, P: platy, B: bladed, E: elongate and V: very. Diagram generated after Graham and Midgley (2000).

TABLE 3. Detection thresholds in three different media.

ENVIRONMENT	MEDIA	AXIS	MAXIMUM DETECTION DEPTH (cm)
Backshore	Pebbles and cobbles	Short	46
		Intermediate	25
		Long	15
Lower foreshore	Sand	Short	35
		Intermediate	21
		Long	17
Submerged beach	Water	Short	22
		Intermediate	16
		Long	13.5

(Fig. 5B) are those with higher recovery rates (Fig. 11). However, the category corresponding to tracers in the range between -5.5 and -6Ø (45.3–64mm) has the most negative slope, and therefore this is the least favourable size range for long-term RFID experiments.

Regarding the different shapes of the tagged particles, no clear pattern is seen when they are plotted against time, despite the great diversity of shapes (Figs. 5C and 7). All shapes present a negative slope, which corresponds to a decrease in the recovery rate. The only difference is that platy and elongate particles show a more stable trend. Therefore, these are the best shapes for this kind of experiment (Fig. 12).

Factors related to the environment

One of the environmental variables to be considered when analyzing the recovery rates of tracers is the wave climate. However, to cope with this effect it is necessary to know what was the time elapsed during which waves were responsible for tracer movement. Four different cases have been considered: the average of hourly wave data during 1, 5, 10 and 20 days prior to the field experiment.

Figure 13 shows the number of recovered particles *vs* significant wave height (Hs) for the four mentioned cases. No clear relationship is found for any of them, which indicates that under high waves and in mild conditions the recovery rates were quite similar. Obviously, waves are the

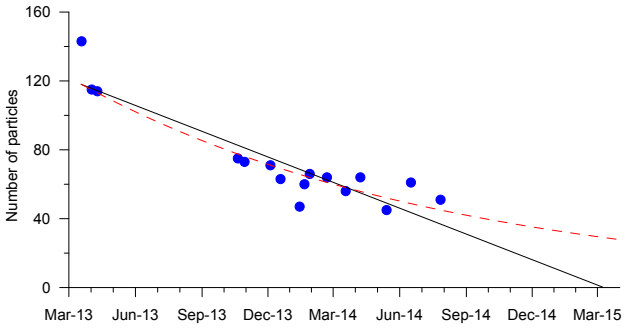

FIGURE 8. Number of particles recovered in each field session. Continues and dashed lines are the linear and exponential fits, respectively. R^2=0.82 in both cases.

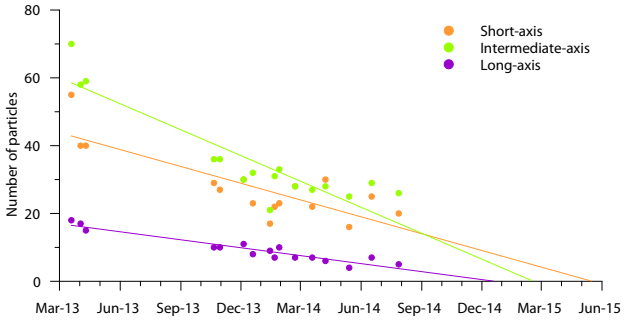

FIGURE 9. Recovered tracers during the time span of the experiment depending on the axis through which the tag was inserted.

main agent of particles movement, but it seems to have no direct effect on tracer recovery.

The second factor to be considered is the elevation of the tracers on the beach. For this purpose we divided the beach into four regions. Tracers found below 0m were below mean low level , those between 0–2m were along the lower and central part of the foreshore, particles between 2–4m were in the upper foreshore and the summer berm, and those above 4m were above the crest of the winter berm. Despite the general decreasing trend in the number of retrieved particles, we found a positive trend for tracers found above 4m (Fig. 14).

DISCUSSION

The entire process of tracer preparation is associated with a certain mass loss of the sample due to the drilling for the tag introduction. It has been calculated that this loss of weight only represents 0.42% on average of the mass of the whole particles (Table 2). This result is similar to that of Miller *et al.* (2011), who state that mass loss after RFID placement in most cases was less than 1%. Therefore, it can be considered that this process does not affect the basic characteristics of the particles.

Results of the detection threshold in depth (Table 3) match those presented by Bertoni *et al.* (2010) who obtained a detection range of 0.40m and 0.35m under water, as well as those from Curtiss *et al.* (2009) who obtained a detection range of 0.40m. However, other authors such as Allan *et al.* (2006) and Dickson *et al.* (2011) obtained ranges from 0.8 to 1m. The detection depth in water is lower than that in other media (sand, gravel), since the signal attenuation in water depends on the frequency of the electromagnetic field and the water conductivity (Bertoni *et al.*, 2010). Therefore, results show that the type of media where the tracer was immersed produces a decrease in the detection threshold in depth. However, Chapuis *et al.* (2014) concluded that the sediment material does not hinder the signal transmission

and thus burial does not significantly affect detection other than to increase the vertical distance between the transponder and the antenna. One of the most important technical factors that could determine the detection threshold is the diameter of the antenna. Allan *et al.* (2006) indicate that reducing the antenna diameter by 70% causes a decrease in surface detection distance of about 50%. Since the different authors use antennas of different diameter sizes, this could explain the different detection thresholds. Nevertheless, there are some other antenna characteristics that are determinant in detection, such as the copper wire diameter, the number of loops and the voltage. None of these have been considered in this paper.

Another important aspect that affects the detection threshold is the tag orientation inside the pebble. Most authors normally obtain higher detection distances (both at surface and at depth) when the tag is perpendicular to the beach surface, which indicates that this is the most favourable position, and this is achieved when the tag is inserted in the short-axis of the particle (Allan *et al.*, 2006; Dickson *et al.*, 2011; Chapuis *et al.*, 2014). The tests we have carried out to calibrate the instrumentation follow the same pattern (Table 3), and the same result was found when the recovery rate obtained from the sixteen field experiments was related to the axis through which the tag was inserted (Fig. 9). Therefore, it is confirmed that particles with tags inserted through the short-axis are more efficient as tracers, since they can be detected when buried in deeper positions and, additionally, they may be recovered after longer periods.

During the first five days the decrease in detection rate was very high: 27.8% in 5 days, 5.6% every day. Between March 19 and April 2, 2013, the decrease in recovery rate was not so strong: 14.1% in 14 days, 1% daily. During the last period the recovery rate was 39% in October 2013 and 26% in July 2014, with a reduction of 0.05% daily. This pattern seems to indicate that certain stability in the recovery rate could be reached if the experiment would continue long enough.

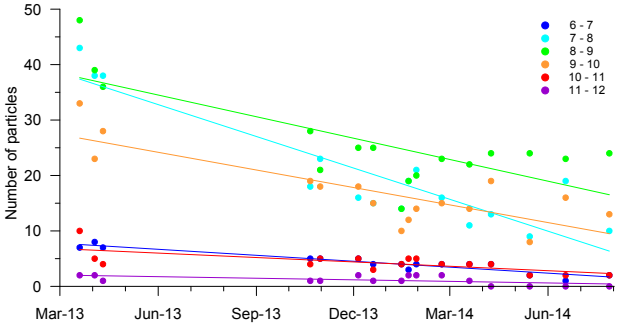

FIGURE 10. Time evolution of the number of recovered particles for the different weight categories (Øw).

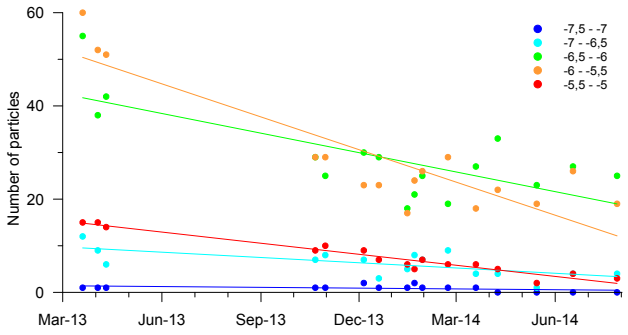

FIGURE 11. Recovered particles for each field session as a function of the length of the intermediate-axis.

Three main possible factors may explain the decrease of recovery rates with time: i) tracers may have been transported out of the survey area; ii) tracers may become buried at greater depths than the detection threshold; and iii) tracers may eventually be destroyed due to abrasion or collision against other particles. Since detected pebbles are not always the same, the stability we have found in the last period could indicate that after a certain period tracers become completely distributed in the three dimensions (alongshore, cross-shore, and in depth). Probably, most tracers that were not retrieved were outside of the survey area or too deeply buried, but they were still active and may eventually be moved again to the survey area. Therefore, the arrival of tracers that were located too far away is compensated by the exit of other tracers that were in the survey area and, as a result, it is possible to achieve certain stability in the number of retrieved particles.

In this study 51 tracers were found seventeen months after deployment, which represents a 25.8% recovery rate. This value is very similar to that of Allan *et al.* (2006), who obtained 24% and 25% recoveries at the lower and upper beaches respectively on the high-energy Oregon coast (USA) after eighteen months. Bertoni *et al.* (2010) obtained 77% two months after tracer deployment, while Curtiss *et al.* (2009) obtained recovery rates higher than 80%, with a minimum of 73% fourteen months after the

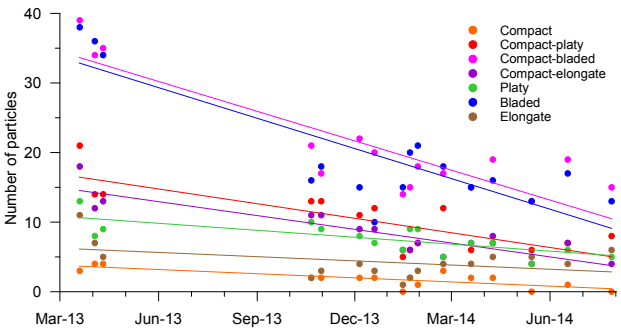

FIGURE 12. Recovered tracers as a function of particle shape.

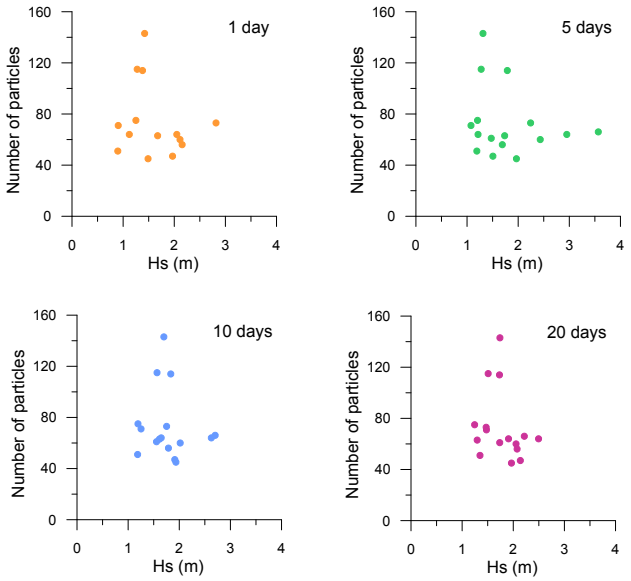

FIGURE 13. Relationship between recovered particles and average significant wave height (Hs) for the four considered cases.

gravel release. Nevertheless, comparison of data is not easy, since the factors that must be taken into consideration include not only the time duration of the experiment, but also the number of storms that occurred and the presence of protective structures on the beach (Benelli *et al.*, 2012). Considering these variables, only the results from Allan *et al.* (2006) are comparable to ours, since the work by Bertoni *et al.* (2010) was carried out on a beach between lateral groins and bounded seaward by a submerged breakwater, and the study site of Curtiss *et al.* (2009) was a mixed sand gravel beach located near a narrow navigation channel, which is completely different to the open ocean beach of San Felipe.

In this study it has been found that there is no significant influence of particle weight and size on the recovery rate (Figs. 10 and 11), since both large and heavy cobbles, as well as small and light pebbles, show a decrease in recovery rates with time. Nevertheless, results obtained in this paper indicate that particles between 7 and 8Øw, as well as those between -5.5 and -6Ø, have the less favourable weights and sizes for long-term RFID experiments. This result agrees with Osborne (2005), who reported a very significant decrease in the recovery rate for small particles. He explained his results arguing that the smaller particles were more favourable for burial than the larger ones, and therefore more difficult to be detected.

Tracer detection rates are higher at the upper part of the beach profile than below the berm (Fig. 14). This pattern is related to particle transport, since those located along the lower part of the profile are more heavily pulled by waves, so that they can be moved larger distances, and some of them may eventually leave the survey area. On the contrary, it is more difficult for particles above the berm to be moved by waves, and therefore they remain in the same location. However, those tracers located close to the berm crest may fall down to the lower part due to berm retreat. Despite this process, the linear fit for particles retrieved at >4m elevation (Fig. 14) shows a positive slope, which indicates that the number of particles retrieved above the berm is gradually increasing. This can only be explained by onshore transport from the foreshore.

Regarding the effect of waves, even though wave energy is the most important agent of particle transport, no clear relationship with recovery has been found. Wave conditions have been very changeable over time, with significant storms during the experiment (see Fig. 4), but the number of detected particles was quite stable. This is in disagreement with Benelli *et al.* (2012), who state that the frequency of storms is a key factor in recovery rates.

CONCLUSIONS

The RFID system developed for this study is based on that of Allan *et al.* (2006) and has proved to be appropriate because it allows to locate tracers accurately and with acceptable recovery rates. Therefore, it permits to study the movement of cobbles and pebbles over long periods of time. The sample preparation process did not affect the basic characteristics of the particles, since the weight loss originated only represented 0.42% of the whole tracers.

After deployment of tracers on the beach, sixteen field experiments were carried out over seventeen months for tracer positioning. Recovery rates strongly decreased at the beginning but tended to stabilize after one year from initial deployment. After seventeen months a recovery rate of 26% was achieved, which is very similar to those reported in the literature for similar periods and open beaches.

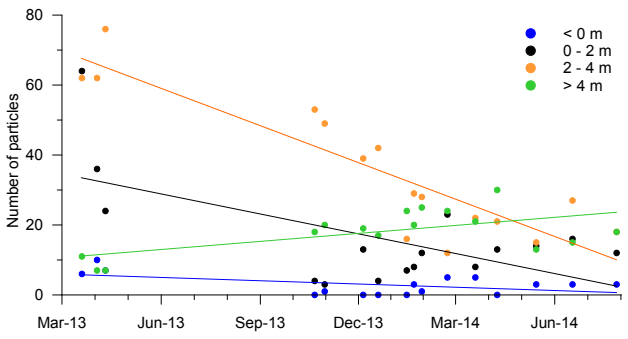

FIGURE 14. Time evolution of the number of recovered tracers as a function of the elevation where they were found.

Several factors that could affect the recovery rate have been considered. Some of them are related to the particle, and it is confirmed that tracers with the tag inserted through the short-axis are more efficient in terms of recovery. Furthermore, the worst particles to be used in RFID long term experiments are those whose intermediate-axis are between -5.5 and -6 Ø, as well as those between 7 and 8 Øw in weight. Regarding particle shape, platy and elongate shapes seem to be the best for this kind of experiment.

Finally, two factors regarding the environmental conditions have been considered. The first was the tracer location of the beach profile found with recovery, and it was clear that the most favorable position to detect a certain tracer is the upper part of the beach, above the storm berm. The second factor was wave energy, and no relationship has been found with recovery rates, which were quite stable both under storm and calm conditions.

ACKNOWLEDGMENTS

We are grateful to the people that participated in the field experiments for their invaluable help. Thanks are due to two anonymous reviewers whose detailed comments have helped to improve this manuscript. Wave data were provided by Pilar Gil from Puertos del Estado.

REFERENCES

Allan, J.C., Komar, P.D., 2004. Environmentally compatible cobble berm and artificial dune for shore protection. Shore and Beach, 72(1), 9-18.

Allan, J.C., Hart, R., Tranquili, J.V., 2006. The use of Passive Integrated Transponder (PIT) tags to trace cobble transport in a mixed sand-and-gravel beach on the high-energy Oregon coast, USA. Marine Geology, 232, 63-86. DOI: 10.1016/j.margeo.2006.07.005

Balcells, R., Barrera, J.L., 1990. Mapa Geológico de España 1:25.000, hoja 1101-III-IV (Arucas). Instituto Tecnológico GeoMinero de España, Madrid.

Benelli, G., Pozzebon, A., Bertoni, D., Sarti, G., 2012. An RFID-based toolbox for the study of under- and outside-water movement of pebbles on coarse-grained beaches. IEEE Journal of selected topic in applied earth observations and remote sensing, 5(5), 1474-1482. DOI: 10.1109/JSTARS.2012.2196499

Bertoni, D., Sarti, G., Benelli, G., Pozzebon, A., Raguseo, G., 2010. Radio Frequency Identification (RFID) technology applied to the definition of underwater and subaerial coarse sediment movement. Sedimentary Geology, 228, 140-150. DOI: 10.1016/j.sedgeo.2010.04.007

Bertoni, D., Sarti, G., Benelli, G., Pozzebon, A., Raguseo, G., 2012. Transport trajectories of "smart" pebbles on an artificial coarse-grained beach at Marina di Pisa (Italy): Implications for beach morphodynamics. Marine Geology, 291-294, 227-235. DOI: 10.1016/j.margeo.2011.08.004

Blair, T.C., McPherson J.C., 1999. Grain-size and textural classification of coarse sedimentary particles. Journal of Sedimentary Research, 1, 6-19. DOI: 10.2110/jsr.69.6

Bray, M.J., Workman, M., Smith, J., Pope, D., 1996. Field measurements of shingle transport using "electronic" tracers. Proceedings 31st Ministry of Agriculture, Fisheries and Food Conference of River and Coastal Engineers. Keele University, United Kingdom, 10.4.1-10.4.13.

Carter, R.W.G., Orford, J.D., 1984. Coarse clastic barrier beaches: a discussion of the distinctive dynamic and morphosedimentary characteristics. Marine Geology, 60, 377-389. DOI: 10.1016/0025-3227(84)90158-0

Chapuis, M., Bright, C.J., Hufnagel, J., MacVicar, B., 2014. Detection ranges and uncertainty of passive Radio Frequency Identification (RFID) transponders for sediment tracking in gravel rivers and coastal environments. Earth Surface Processes and Landforms, 39, 2109-2120. DOI: 10.1002/esp.3620

Ciavola, P., Castiglione, E., 2009. Sediment dynamics of mixed sand and gravel beaches at short time-scales. Journal of Coastal Research, Special Issue 56, 1751-1755.

Curtiss, G.M., Osborne, P.D., Homer-Devine, A.R., 2009. Seasonal patterns of coarse sediment transport on a mixed sand and gravel beach due to vessel wakes, wind waves, and tidal currents. Marine Geology, 259, 73-85. DOI: 10.1016/j.margeo.2008.12.009

Dickson, M.E., Kench, P.S., Kantor, M.S, 2011. Longshore transport of cobbles on a mixed sand and gravel beach, southern Hawke Bay, New Zealand. Marine Geology, 287, 31-42. DOI: 10.1016/j.margeo.2011.06.009

Dornbusch, U., Williams, R.B.G, Moses, C., Robinson, D.A., 2002. Life expectancy of shingle beaches: measuring in situ abrasion. Journal of Coastal Research, Special Issue 36, 249-255.

Graham, D.J., Midgley, N.G., 2000. Graphical representation of particle shape using triangular diagrams: an excel spreadsheet method. Earth Surface Processes and Landforms, 25, 1473-1477. DOI: 10.1002/1096-9837(200012)25:133.0.CO;2-C

Jolliffe, I.P., 1964. An experiment designed to compare the relative rates of movement of different sizes of beach pebble. Proceedings of the Geologists Association, 75, 67-86. DOI: 10.1016/S0016-7878(64)80012-2

Krumbein, W.C., 1936. Application of logarithmic moments to size-frequency distributions of sediments. Journal of Sedimentary Research, 6(1), 35-47. DOI: 10.1306/d4268f59-2b26-11d7-8648000102c1865d

Menéndez, I., Silva, P.G., Martín-Betancor, M., Pérez-Torrado, F.J., Guillou, H., Scaillet, S., 2008. Fluvial dissection, iostatic uplift, and geomorphological evolution of volcanic islands (Gran Canaria, Canary Islands, Spain). Geomorphology, 102, 189-203. DOI: 10.1016/j.geomorph.2007.06.022

Miller, I.M., Warwick, J.A., 2012. Measuring sediment transport and bed disturbance with tracers on a mixed beach. Marine Geology, 299-302, 1-17. DOI: 10.1016/j.margeo.2012.01.002

Miller, I.M., Warwick, J.A., Morgan, C., 2011. Observations of coarse sediment movements on the mixed beach of the Elwha Delta, Washington. Marine Geology, 282, 201-214.

DOI: 10.1016/j.margeo.2011.02.012

Osborne, P.D., 2005. Transport of gravel and cobble on a mixed-sediment inner bank shoreline of a large inlet, Grays Harbor, Washington. Marine Geology, 224, 145-156. DOI: 10.1016/j.margeo.2005.08.004

Sear, D.A., Lee, M.W.E., Oakey, R.J., Carling, P.A., Collins, M.B., 2002. Coarse sediment tracing technology in littoral and fluvial environments a review. In: Foster, I. (ed.) Tracers in the environment. Chichester (UK), Earth Surface Processes and Landforms, Wiley and Sons, Special Issue, 21-55.

Sneed, D., Folk, R.L., 1958. Pebbles in the Lower Colorado River, Texas a study in particle morphogenesis. The Journal of Geology, 66(2), 114-150. DOI: 10.1086/626490

Voulgaris, G., Workman, M., Collins, M.B., 1999. Measurement techniques of shingle transport in the nearshore zone. Journal of Coastal Research, 15(4), 1030-1039.

Manuscript received November 2013;
revision accepted December 2014;
published Online May 2015.